# A dynamical attractor governs beach response to storms

Nathaniel G. Plant,[1] K. Todd Holland,[1] and Rob A. Holman[2]

Received 5 June 2006; accepted 10 August 2006; published 9 September 2006.

[1] Sandbars are ubiquitous, yet not well understood beach features that change their position and shape in response to changing wave conditions. We propose and test a simple empirical model consisting of two coupled linear differential equations that represents bar dynamics in terms of wave forcing and two other state variables: (1) the mean cross-shore bar position and (2) the alongshore variability about that mean. Model coefficients are constrained by fitting to a 2-month data set, and the modeled behavior is examined with a stability analysis. The system is found to be stable and, hence, predictable. Rates of change of the bar position and its alongshore variability are found to be significantly coupled, such that prediction of one variable requires information about the other. The system response time is slow compared to the storm wave cycle such that the bar response continually orbits time-varying equilibrium points in the state variable phase plane. **Citation:** Plant, N. G., K. T. Holland, and R. A. Holman (2006), A dynamical attractor governs beach response to storms, *Geophys. Res. Lett.*, *33*, L17607, doi:10.1029/2006GL027105.

## 1. Introduction

[2] It is somewhat counter-intuitive that unconsolidated sand, resting on an ocean beach under the action of ocean waves, will typically form a beach profile that is not monotonic, but instead features one or more local shallows called sand bars. Observations from a variety of locations show that beaches with bars are common [*Plant et al.*, 1999; *Ruessink et al.*, 2003; *Alexander and Holman*, 2004]. Moreover, the horizontal planform (or morphology) of sand bars can vary substantially, from those with no alongshore variation (linear bars) through a variety of patterns that can be quasi-periodic or even irregular [*Sonu*, 1973; *Wright and Short*, 1984; *Lippmann and Holman*, 1990].

[3] A particularly clear example of sandbar response, which also serves as the data set for this paper, was observed during Hurricane Bonnie from the period 01 August 1998 to 30 September 1998 at the Army Corps of Engineers' Field Research Facility, near the town of Duck, N.C., USA. The cross-shore position and alongshore variation of a nearshore sandbar were monitored using time-averaged video imagery (Figure 1) obtained from seven cameras mounted on a 43 m high tower. White foam produced as waves break in the relatively shallow water over sandbars is used to reveal bar position and shape [*Lippmann and Holman*, 1989]. Bonnie produced offshore wave heights of nearly 3 m (Figure 2a). Beginning a few days prior to the hurricane's landfall, a clearly identifiable sandbar with some minor alongshore irregularity was located about 50 m offshore (Figure 1a); then, this bar migrated about 25 m offshore in association with the largest storm waves (Figure 1b). Over the subsequent 2 weeks, the alongshore-uniform sandbar developed into a chain of crescentic bars that migrated slowly onshore (Figure 1c).

[4] This sequence of response has been widely observed elsewhere [*Short*, 1975; *Wright et al.*, 1985; *Lippmann and Holman*, 1990; *Ranasinghe et al.*, 2004] and the recognizable bar patterns have been called morphodynamic states with names like "longshore bar-trough" (Figures 1a and 1b) and "rhythmic" (Figure 1c) that can form a discrete basis set of morphology descriptors. Transitions between states are assumed to occur at threshold values of some variable (perhaps wave height or a combination of wave and sediment parameters), and each state is assumed to instantly respond to and exist in equilibrium with, for example, a particular range of wave heights [*Wright et al.*, 1985; *Lippmann and Holman*, 1990]. Typically predictions from this class of models have not been accurate [*Sonu and James*, 1973; *Ranasinghe et al.*, 2004], which we hypothesize is, in part, due to the unmodelled feedback mechanisms and discrepancies between the longer response time scale of sand bars and the shorter time scales of variation of wave forcing.

[5] A number of existing models address the time evolution of arbitrary sand bar profiles by coupling sediment transport models with measurements of relevant flow properties [e.g., *Thornton et al.*, 1996; *Gallagher et al.*, 1998; *Hoefel and Elgar*, 2003; *Henderson et al.*, 2004]. While explicitly recognizing the dynamic nature of the system and producing skillful predictions (when compared to measured profile change), these and other models do not explicitly examine the feedback between the hydrodynamic and bathymetric components of the sand bar system. In particular, these models assume that alongshore variability is either unimportant or adequately captured by the measured flow properties that sample only the 1-D (cross-shore) dynamics. These models do not address the possible role that the commonly-observed alongshore variations of bathymetry (e.g., Figure 1c) and the resulting circulation may have on sediment transport balances.

[6] Here, we take a different, macroscopic approach and use a dynamical feedback model to capture both the response of sandbars to wave forcing as well as the coupling between the mean sand bar position and alongshore variations in that position (and the associated hydrodynamics, by inference). We use observations to constrain the feedback model and describe the system's stability and behavior. Alongshore variations in bar crest

[1] Naval Research Laboratory, Stennis Space Center, Mississippi, USA.
[2] Coastal Imaging Lab, Oregon State University, Corvallis, Oregon, USA.


0094-8276/06/2006GL027105$05.00

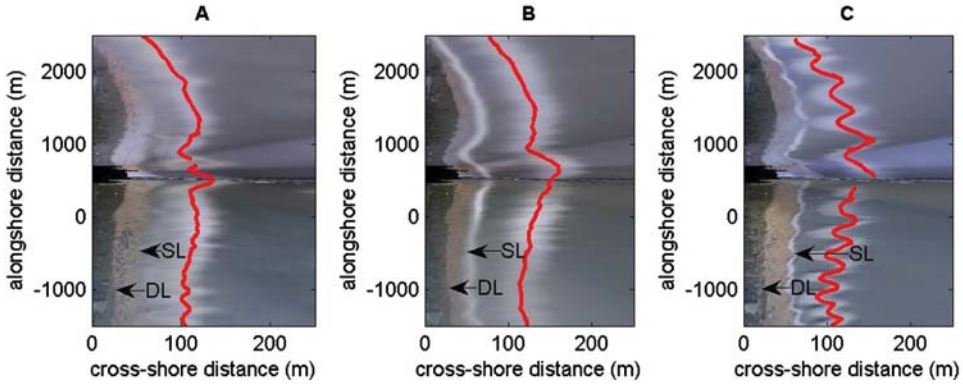


**Figure 1.** Mapped imagery of nearshore region (with substantial cross-shore exaggeration) for 23 and 28 August (a, b) and 9 September (c). Red line indicates bar positions estimated for each image. A pier is visible in the central region of each image, extending across the entire domain (this region was omitted from the analysis). Arrows indicate the shoreline (SL, where the dry beach meets the water) and the dune line (DL, where the beach ends).

position are found to play an important role in mean bar position response.

## 2. Theory

[7] The preponderance of published results showing beaches returning to recognizable morphodynamic states supports the idea that sandbar patterns are driven by negative feedback toward some sort of time-varying equilibrium. But, it is also possible that the system exhibits unexpected behavior due to feedback between its different components. We propose a simple model for predicting horizontal bar response where the change in the along-shore mean bar position, $x$, and change in the horizontal amplitude of the alongshore-variable component of the bar pattern, $a$, depend on each other and on the incident wave height in the following linearized feedback model

$$\begin{bmatrix} \dot{x} \\ \dot{a} \end{bmatrix} = A \begin{bmatrix} x \\ a \end{bmatrix} + B \begin{bmatrix} 1 \\ F \end{bmatrix}. \tag{1}$$

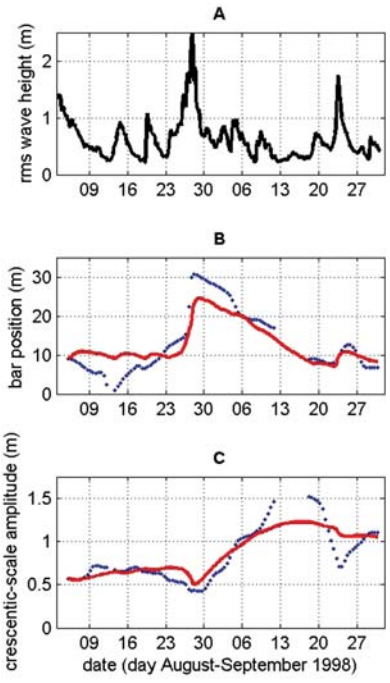


**Figure 2.** (a) Time series of wave height measured in 8 m water depth, about 1 km offshore. (b) Observed (dots) and predicted (solid line) bar position and (c) amplitude of the crescentic-scale alongshore variability. A bar position of zero corresponds to the minimum observed position.

[8] The matrix A describes the interaction between $x$ and $a$, and $F$ is a forcing function here chosen to be a function of the offshore root mean square wave height ($H_{rms}$): $F(t) = [H_{rms}(t)]^p$. The matrix B describes the linear response of the system to the forcing plus a constant that accounts for non-zero mean values of $x$ and $a$.

[9] Our model does not explain the existence of bars, the particular length scale of alongshore variability that might occur, or any details of the fluid dynamics or sediment transport over the bar system. Instead it explores the macroscopic variability of the state variables and the nature and consequences of feedback between the variables. Typically, nonlinear models have been used to reveal interesting dynamics in many science fields, ranging from biology [*May*, 1976] to meteorology [*Lorenz*, 1984]. While the behavior of an actual bar system is most likely very nonlinear [*Reniers et al.*, 2004], the linear approximation (equation 1) admits both stable (i.e., equilibrium-seeking) and unstable dynamics. The form of equation 1 is typically used in prediction and control theory [*Kalman*, 1960] and has been chosen here to facilitate a straightforward stability analysis of the sandbar dynamics. The approach has been applied successfully in analysis of tidal morphodynamics [*van Goor et al.*, 2004] and it can be fruitful even if the interactions captured by matrix A are only qualitatively accurate [*Phillips*, 1992].

[10] The nature of the dynamics of the model (equation 1) is completely determined by the particular values of the interaction coefficients (matrix A) and forcing coefficients (matrix B). These values are obtained by fitting to observations. With coefficients established, the equilibrium values ($x_0$, $a_0$) for any particular value of forcing can be

computed by setting the left hand side of equation (1) to zero:

$$\begin{bmatrix} x_0 \\ a_0 \end{bmatrix} = -[A]^{-1}B\begin{bmatrix} 1 \\ F \end{bmatrix} \equiv B_0\begin{bmatrix} 1 \\ F \end{bmatrix}. \tag{2a}$$

[11] The equilibrium values are a linear function of the forcing (equation 2a). The equilibrium state is called an attractor and the system is stable if the dynamics drive the bar components towards equilibrium.

[12] To find out whether the system is stable or unstable, a perturbation (such as might be introduced by a change in wave conditions) can be assumed to exhibit exponential growth with a timescale of $\lambda$:

$$\begin{bmatrix} x - x_0 \\ a - a_0 \end{bmatrix} = \begin{bmatrix} \xi \\ \alpha \end{bmatrix} e^{\lambda t}. \tag{2b}$$

[13] This leads to an eigenvalue problem

$$\lambda\begin{bmatrix} \xi \\ \alpha \end{bmatrix} = A\begin{bmatrix} \xi \\ \alpha \end{bmatrix}, \tag{3}$$

where $\lambda$ are eigenvalues of the corresponding system (equation 3), with eigenvectors $\xi$ and $\alpha$. The sign of the real part of $\lambda$ dictates the stability of this system; the presence of an imaginary component indicates oscillation. The eigenvectors describe the nature of the coupled response between bar position and crescentic amplitude.

## 3. Methods

[14] Imagery was obtained from five collocated cameras (data available on http://cil-www.oce.orst.edu/argus02a/1998/, cameras c0–c4) that provided a panoramic view of the coast. The raw imagery was processed on site to produce time-exposure images, which removed rapidly fluctuating features (such as individual waves) that vary over a 10 minute averaging period. Using standard photogrammetry, the images were projected to a plane located at sea level, and then the images were merged at hourly (daylight) intervals into a series of maps (Figure 1). Using a well established approach for finding nearshore features [*Plant and Holman*, 1997; *van Enckevort and Ruessink*, 2003], the bar location as a function of alongshore position was identified in the maps at 50 m spacing. Remote sensing artifacts due to tide and wave height variations were corrected by interpolating bar positions to mean tide level and mean wave height. (The tide and wave height data are available on http://www.frf.usace.army.mil/.) Interpolation was performed over time and space, removing variations with an alongshore length scale <100 m and time scale <3 days. Interpolation errors were computed [*Plant et al.*, 2002] in order to determine the reliability of bar position estimates. This procedure produced one estimate of the cross-shore bar position as a function of alongshore coordinate at 0.5 day intervals. From these data, the alongshore averaged (over the 4 km study area) bar position, $x$, and crescentic-scale amplitude, $a$, were computed for each time interval. While the term crescentic is used here for convenience, we make no requirement on actual bar shape and define $a$ as the root mean variance in the band 200 m < L < 1000 m, obtained from an alongshore Fourier decomposition of bar position data.

[15] The coefficient matrices A and B were estimated by integrating equation 1 over successive 0.5 day intervals and fitting the model to the observed changes in $x$ and $a$ using linear regression. Out of 121 observations, 21 were rejected because the interpolation procedure failed to achieve an 80% reduction in sampling errors. The best prediction skill of the model resulted from p = 2 (using 0,1,2,3 as trials for p). The skill was tested by initializing the model with the first observations of $x$ and $a$ and then driving the model forward with observed wave heights (Figures 2a, 2b, and 2c). The skill ($R^2$) of 0.9 was significant at the 95% confidence level.

## 4. Results

[16] The estimated coefficients for the Hurricane Bonnie data set were

$$A = \begin{bmatrix} -0.071 \pm 0.03\left[\mathbf{d}^{-1}\right] & -0.70 \pm 1.0\left[\mathbf{d}^{-1}\right] \\ 0.0047 \pm 0.001\left[\mathbf{d}^{-1}\right] & -0.022 \pm 0.03\left[\mathbf{d}^{-1}\right] \end{bmatrix},$$

$$B = \begin{bmatrix} 0.50 \pm 1.0\left[\mathbf{md}^{-1}\right] & 2.1 \pm 0.4\left[(\mathbf{md})^{-1}\right] \\ -0.014 \pm 0.03\left[\mathbf{md}^{-1}\right] & -0.040 \pm 0.01\left[(\mathbf{md})^{-1}\right] \end{bmatrix},$$

where the uncertainty indicates the standard deviation of the estimated values (not the standard error). Several broad conclusions can be made. The negative values on the diagonal of A (the self-interaction terms) indicate a stabilizing tendency because a positive perturbation produces a negative response and vice versa. If the diagonal terms are both negative, the off-diagonal cross interaction terms do not change the stability of the system so long as they have opposite signs, as is the case in our example. (Or, at least this is the most likely situation given the uncertainty in the parameter estimation.) The values in the second column of B describe how different wave heights affect the bar response. In the absence of coupling, an increase in wave height would drive positive changes in bar position and negative changes in crescentic amplitude. However, after accounting for the coupling by computing $B_0$, we find that the equilibrium crescentic amplitude actually increases with increasing wave height, i.e.,

$$\begin{aligned} x_0 &= 4.28 + 14.95F \\ a_0 &= 0.28 + 11.26F. \end{aligned} \tag{4}$$

[17] The solution of the eigenvalue problem (equation 3) yielded a complex eigenvalue ($\lambda = -0.05 \pm 0.05$i). The sign of the real part of the eigenvalue is negative, indicating that the system is stable. If the forcing is held constant and the system is perturbed, the bar position and amplitude will return to equilibrium with a decay timescale of $\Re(\lambda)^{-1}$, or about 20 days. The imaginary part of the eigenvalue indicates that an oscillation is superposed upon the exponential decay. The period of this oscillation, $T = (2\pi)\Im(\lambda)^{-1}$, which is about 120 days, is long compared to the decay time scale such that when bar position and amplitude are plotted as trajectories in a phase portrait

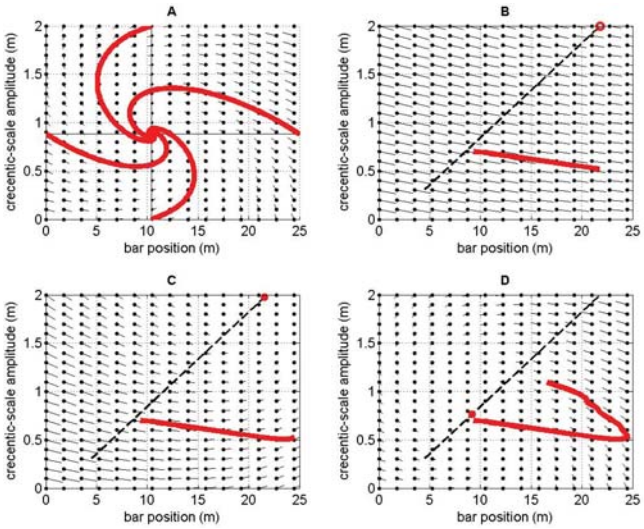


**Figure 3.** Phase portraits. The sticks (whose origins lie on a regular grid of dots) point in the direction of dynamical flow corresponding to a particular wave height. (a) Hypothetical situation for constant wave height equal to the mean value (0.64 m). Spiraling curves show the modeled trajectories for several different initial conditions converging at the equilibrium state. (b–d) Phase portraits corresponding to observed wave height on 28 August (Figure 3b), 29 August (Figure 3c), and 9 September (Figure 3d). A straight dashed line marks the locus of all equilibria and the particular equilibrium state for each phase portrait is marked with a filled circle that falls on that line. (The open circle in Figure 3b indicates that the equilibrium state does not lie within the domain.) The modeled trajectory (curve, updated in each phase portrait) was initialized at the observed state on 23 August and driven by the time-varying wave height.

(Figure 3a) the system is shown to return to equilibrium along a spiraling path. The oscillations will be heavily damped before completing even one cycle.

[18] The nature of the response is further characterized by the complex eigenvectors ($\xi = -1.00$, $\alpha = 0.04 \pm 0.07i$), which describe the relative magnitudes and a phase shift of bar position and crescentic amplitude response. The difference in magnitudes of the vector components is proportional to the observed difference in variability of bar position and amplitude response (Figures 2b and 2c). The complex phase shift ($\phi = \mathrm{Tan}^{-1}[\Im(\alpha/\xi)/\Re(\alpha/\xi)]$) indicates how a perturbation in one component drives a response in the other. A phase shift of 0 indicates no interaction between bar position and crescentic amplitude, while a phase shift of 90 degrees (quadrature) means a perturbation in bar position will drive a response only in the amplitude. The estimated phase shift was 115 degrees, indicating partial quadrature. For example, if a sandbar's crescentic amplitude is at equilibrium but the bar position is displaced offshore of its equilibrium (see Figure 3a), the bar position will have a negative response (onshore migration) and the amplitude has a positive response (amplitude increase). The amplitude change will then feed back into the response of the bar position, thereby deflecting the trajectories away from any direct path toward equilibrium.

## 5. Discussion

[19] These results lead to several important conclusions. First, the dynamics of the modeled sand bar system are stable. This implies that time series of the coupled bar position-amplitude system are inherently predictable, even if the wave conditions are changing (Figures 2a, 2b, and 2c). Figures 3b–3d show how the time series were modeled using the observed wave height. The time-varying forcing caused the equilibrium state of the system to vary. The bar position and crescentic amplitude responses adjust to the variations, but their relatively slow response, compared to changes in the wave height, does not allow them to reach equilibrium.

[20] Second, this analysis indicates that feedback between bar position and the crescentic amplitude is important. Specifically, the cross-interaction is important such that bar migration depends strongly on amplitude and vice versa. The cross-interaction is responsible for the spiraling approach towards equilibrium and explains the hysteresis associated with observed morphologic state changes. That is, an increase in wave height (a storm) may drive a sandbar offshore and, initially, cause a reduction in crescentic amplitude. At this point, if the wave height decreases (the storm has passed), the bar will not reverse its response (first migrate onshore, then increase amplitude), but will instead immediately experience an increase in amplitude and then slowly migrate onshore. For instance, Figure 3b shows offshore migration and a decrease in amplitude driven by a relatively short-lived increase in wave height. This response is consistent with previous interpretations of bar behavior during storms and is consistent with the data used in this study (Figures 2b and 2c). Continuing through the sequence as the wave height drops rapidly from 2 m (Figure 3b) to 1 m (Figure 3c) to less than 1 m (Figure 3d), we predict an increase in crescentic amplitude and onshore migration. The modeled response orbits around the changing equilibrium points in the phase portrait, reflecting the complicated interaction between sandbars, waves, and circulation patterns driving sediment transport.

[21] The analysis of the dynamics was largely unchanged by varying by one standard deviation the estimated interaction terms in the matrix A. This suggests that the parameter estimates were sufficiently accurate to characterize the system dynamics. Only in one case, where the sign of the term $A_{12}$ changed from $-0.7$ (alongshore variability drives onshore bar migration) to 0.3 (alongshore variability drives offshore bar migration), was there a qualitative change in the system dynamics. With the sign change in this parameter, the corresponding stability analysis predicted strongly stable response only if perturbations of the bar and alongshore variability had opposite signs (e.g., bar position offshore of equilibrium and alongshore variability smaller than equilibrium). If perturbations of bar position and alongshore variability had the same sign (e.g., bar offshore of equilibrium and large alongshore variability), weakly stable response was predicted with a response time of 100 days. The possibility for the bar system's stability to depend on the system state is an interesting concept, but it is not one that can be addressed with the present data set.

[22] We must emphasize that our results characterize a particular realization of sandbar response with the assumption that the model (equation 1) describes small perturba-

tions from some mean state. If there are large variations in the mean bar position, or in the characteristic length scale of the alongshore variations, or in some un-modeled component of the system (such as wave period or direction), then the model coefficients might need to be re-evaluated. For instance, it is well documented that there is an offshore bar at the study site (located at a cross-shore coordinate ranging between 300 m and 400 m), that periodically disappears, affecting the wave conditions at the inner bar that was the focus of this study. Specifically, *Plant et al.* [1999] analyzed several decades of bar position data and found different characteristic response times for inner and outer bars. (They also found that a response time that varied with wave height was required to explain an inter-annual trend of offshore bar migration. To apply this to our analysis would require that the parameters in the interaction matrix vary with wave height. It appears that this is not necessary to capture the important dynamics of our shorter term analysis of much smaller perturbations to the bar system.) Application of the present analysis approach to a different geographic location, where there might be significantly altered details of wave, current, and sediment transport processes, would also require re-evaluation of the model parameters, with the possibility of identifying different system dynamics.

[23] The observed link between horizontal variability in bar morphology (and, presumably, the associated flow circulation) and the rate of onshore bar migration may be of more than academic interest. Current attempts to model cross-shore bar migration almost invariably assume 1-D dynamics, wherein the dominant physics can everywhere be modeled in terms of cross-shore balances involving hydrodynamics over a previous beach profile and the changes of that profile due to induced sediment transport. The results from this paper suggest that horizontal circulation may play an important role, particularly in facilitating onshore transport and bar movement after storms. Two-dimensional flow and sediment transport models exist [*Falques et al.*, 2000; *Reniers et al.*, 2004], but they have not yet demonstrated significant predictive skill in comparisons to field observations. This suggests that the dominant feedback mechanisms are, as yet, inaccurately parameterized in these detailed coupled models.

[24] Finally, the predicted equilibrium state varies with changes in wave height in an unexpected way. While this and previous studies predict that the equilibrium bar position moves offshore with increasing wave height, the present model predicts that the equilibrium crescentic amplitude increases with increasing wave height (equation 4, Figures 3b–3d). This is opposite to conclusions from previous studies [*Wright and Short*, 1984; *Ranasinghe et al.*, 2004], which suggest that the observed reduction in amplitude during storms meant that the equilibrium state must include long straight bars. We emphasize that these conclusions relate only to equilibrium states (which appear to be largely unreachable) and note that the observed and modeled amplitudes in this study (Figure 2c), which were not at equilibrium, show a decrease in amplitude immediately following the storm. Direct observation of equilibrium is missing because the wave height subsides rapidly after a passing storm. In support of the present model's prediction, we note that a geometric constraint is imposed by the shoreline, limiting the crescentic amplitude as a bar approaches the shore. Because the equilibrium bar position increases with increasing wave height and the amplitude is coupled to the bar position, the equilibrium amplitude may be enslaved to both the bar position and shoreline constraints.

## 6. Conclusions

[25] A simple, empirical dynamical model of sand bar behavior is presented that represents the macroscopic dynamics in terms of two, coupled differential equations describing the evolution of the alongshore mean ($x$) and alongshore, band-limited standard deviation ($a$) of sand bar position. Each equation is driven by a time-varying wave forcing and each allows interactions between the variables to occur. In contrast to equilibrium bar models whose tests are confused by the need to make arbitrary assumptions of an averaging time scale for wave forcing, time evolution is handled naturally and the system need never approach equilibrium. After a least squares solution for system coefficients based on two months of observations, examination of the system stability revealed several important properties. The dynamics were found to be stable, indicating a tendency for the system to return to equilibrium—a result that is consistent with previous interpretations and that also suggests that the system is inherently predictable. The two state variables were found to be coupled such that disequilibrium in one also drives variation in the other. For example, under calm conditions, the shoreward migration of the bar must be coupled to a growth of alongshore bar variability and, presumably, the development of horizontal circulation. The idea that horizontal circulation may facilitate onshore migration is a paradigm shift from traditional models that assume one-dimensional dynamics only. Consistent with observations, offshore bar migration under storms is initially associated by a bar straightening. Model predictions of eventual growth of alongshore variability under storms are rarely realized due to the long response time of the bar system compared to that of storms. Overall, the modeled response is a sand bar system that continually orbits time-varying equilibrium points in the state variable phase plane.

[26] **Acknowledgments.** Funding for NGP and KTH provided by Office of Naval Research through base funding to the Naval Research Laboratory, Program Element 0602435N. Funding for RAH was provided by the Office of Naval Research, Geosciences Program, grant N00014-02-1-0154. We are grateful for the data collected by our colleagues at the Army Corps of Engineer's Field Research Facility and we appreciate the useful comments of two anonymous reviewers. Correspondence and requests for materials should be addressed to N.G.P. (e-mail: nplant@nrlssc.navy.mil).

## References

Alexander, P. S., and R. A. Holman (2004), Quantification of nearshore morphology based on video imaging, *Mar. Geol.*, *208*, 101–111.

Falques, A., G. Coco, and D. A. Huntley (2000), A mechanism for the generation of wave-driven rhythmic patterns in the surf zone, *J. Geophys. Res.*, *105*(C10), 24,071–24,087.

Gallagher, E., R. T. Guza, and S. Elgar (1998), Observations of sand bar evolution on a natural beach, *J. Geophys. Res.*, *103*(C2), 3203–3215.

Henderson, S., J. Allen, and P. Newberger (2004), Nearshore sandbar migration predicted by an eddy-diffusive boundary layer model, *J. Geophys. Res.*, *109*, C06024, doi:10.1029/2003JC002137.

Hoefel, F., and S. Elgar (2003), Wave-induced sediment transport and sandbar migration, *Science*, *299*(5614), 1885–1887.

Kalman, R. E. (1960), A new approach to linear filtering and prediction problems, *J. Basic Eng.*, *82*(Ser. D.), 35–45.

Lippmann, T. C., and R. A. Holman (1989), Quantification of sand bar morphology: A video technique based on wave dissipation, *J. Geophys. Res.*, *94*(C1), 995–1011.

Lippmann, T. C., and R. A. Holman (1990), The spatial and temporal variability of sand bar morphology, *J. Geophys. Res.*, *95*(C7), 11,575–11,590.

Lorenz, E. N. (1984), Irregularity: A fundamental property of the atmosphere, *Tellus*, *36A*, 98–110.

May, R. M. (1976), Simple mathematical models with very complicated dynamics, *Nature*, *261*, 459–467.

Phillips, J. D. (1992), Qualitative chaos in geomorphic systems, with an example from wetland response to sea level rise, *J. Geol.*, *100*, 365–374.

Plant, N. G., and R. A. Holman (1997), Intertidal beach profile estimation using video images, *Mar. Geol.*, *140*, 1–24.

Plant, N. G., R. A. Holman, M. H. Freilich, and W. A. Birkemeier (1999), A simple model for interannual sandbar behavior, *J. Geophys. Res.*, *104*(C7), 15,755–15,776.

Plant, N. G., K. T. Holland, and J. A. Puleo (2002), Analysis of the scale of errors in nearshore bathymetric data, *Mar. Geol.*, *191*, 71–86.

Ranasinghe, R., G. Symonds, K. Black, and R. A. Holman (2004), Morphodynamics of intermediate beaches: A video imaging and numerical modelling study, *Coastal Eng.*, *51*, 629–655.

Reniers, A. J. H. M., J. A. Roelvink, and E. B. Thornton (2004), Morphodynamic modeling of an embayed beach under wave group forcing, *J. Geophys. Res.*, *109*, C01030, doi:10.1029/2002JC001586.

Ruessink, B. G., K. M. Wijnberg, R. A. Holman, Y. Kuriyama, and I. M. J. van Enckevort (2003), Intersite comparison of interannual nearshore bar behavior, *J. Geophys. Res.*, *108*(C8), 3249, doi:10.1029/2002JC001505.

Short, A. D. (1975), Three-dimensional beach stage model, *J. Geol.*, *87*, 553–571.

Sonu, C. J. (1973), Three-dimensional beach changes, *J. Geol.*, *81*, 42–64.

Sonu, C. J., and W. R. James (1973), A Markov model for beach profile changes, *J. Geophys. Res.*, *78*, 1462–1471.

Thornton, E. B., R. T. Humiston, and W. Birkemeier (1996), Bar/trough generation on a natural beach, *J. Geophys. Res.*, *101*, 12,097–12,110.

van Enckevort, I. M. J., and B. G. Ruessink (2003), Video observations of nearshore bar behaviour. part 1: Alongshore uniform variability, *Cont. Shelf Res.*, *23*(5), 501–512.

van Goor, M. A., T. J. Zitman, Z. B. Wang, and M. J. F. Stive (2004), Impact of sea-level rise on the morphological equilibrium state of tidal inlets, *Mar. Geol.*, *202*, 211–227.

Wright, L. D., and A. D. Short (1984), Morphodynamic variability of surf zones and beaches: A synthesis, *Mar. Geol.*, *56*, 93–118.

Wright, L. D., A. D. Short, and M. O. Green (1985), Short-term changes in the morphodynamic states of beaches and surf zones: An empirical predictive model, *Mar. Geol.*, *62*, 339–364.

K. Todd Holland and N. G. Plant, Naval Research Laboratory, Stennis Space Center, MS 39529, USA. (nplant@nrlssc.navy.mil)

R. A. Holman, Coastal Imaging Lab, Oregon State University, Corvallis, OR 97331, USA.